ELSEVIER Journal of Electron Spectroscopy and Related Phenomena 101–103 (1999) 665–669

JOURNAL OF ELECTRON SPECTROSCOPY and Related Phenomena

Non-linearity observed in the direct sub-ps photoemission regime in Mo

Gabriele Ferrini[a], Antonio Viggiani[b], Daniele Sertore[b], Paolo Michelato[b], Fulvio Parmigiani[c,*]

[a] *Istituto Nazionale per la Fisica della Materia and Dipartimento di Fisica, Politecnico di Milano, P.za Leonardo Da Vinci 32, I-20133 Milano, Italy*

[b] *Istituto Nazionale di Fisica Nucleare, Laboratorio LASA Via Fratelli Cervi, 201, I-20090 Segrate (Mi), Italy*

[c] *Istituto Nazionale per la Fisica della Materia and Dipartimento di Matematica e Fisica, Università Cattolica, Via Trieste, 17, I-25121 Brescia, Italy*

Abstract

The total charge emitted from a polycrystalline Mo surface by 500 fs–264 nm laser pulses has been measured. Though a one-photon photoelectric effect is expected, a non-linear increase of the photoelectric yield was observed as a function of laser peak intensity, confirming earlier observations on Au, W and Zr. The threshold intensity for this non-linearity is between 0.1 and 0.2 GW/cm^2. The linear and non-linear regimes were clearly discerned in the experimental data. The non-equilibrium heating of the conduction electrons is considered as the cause of the observed non-linear behaviour.

Keywords: Non-equilibrium heating; Photoemission; Short UV laser pulses

1. Introduction

This work explores the effects of non-equilibrium heating [1–3] on the total yield of electron photoemission induced by UV sub-ps laser pulses on polycrystalline Mo. It is found that the predictions of the classical Fowler–DuBridge theory [4,5], extended by Bechtel to the non-equilibrium, high intensity regime (EFD, Extended Fowler–DuBridge theory) [6,7], are consistent with our experimental data. A pure volume photoemission is produced, excluding any contribution from surface enhanced optical absorption [8], by focusing the laser radiation on the sample surface at normal incidence. The linear and non-linear regimes are clearly observed with a threshold intensity between 0.1 and 0.2 GW/cm^2. In addition it is demonstrated that the non-equilibrium heating of the conduction electrons is at the origin of the observed non-linear photoemission behaviour.

2. Experimental

The radiation source, described elsewhere [9], is a laser system capable of emitting UV pulses at 264 nm ($h\nu \cong 4.7$ eV), with a temporal width of about 500 fs and a maximum energy per pulse of 300 μJ. The duration of the UV pulses is measured with a custom designed autocorrelator, based on self-diffraction in a quartz crystal [10]. The spectrum of the

*Corresponding author. Tel.: +39-030-2406-259; fax: +39-030-2406-282.
E-mail address: fulvio@dmf.bs.unicatt.it (F. Parmigiani)

0368-2048/99/$ – see front matter
PII: S0368-2048(98)00333-8

laser pulses is monitored continuously during the experiments, which allows the pulse duration stability to be checked.

The polycrystalline Mo sample is polished with a micrometer powder compound to a mirror finish, cleared in ultra-sonic baths of acetone and ethyl alcohol and dried with N_2. After the insertion in an ultra-high vacuum system (base pressure of 4×10^{-9} mbar during the experiments) the emitting area is activated by irradiating in situ with 264-nm high fluence laser pulses. As reported by other authors [11,12], this provides a satisfactory cleaning action, removing a significant portion of the oxide at the surface, as demonstrated by the observed increase in photoemission yield with laser irradiation.

A 2-mm diameter iron wire is mounted in front of the sample surface at a distance of about 3 mm and biased to 11 kV to work as an anode and to collect the photoemitted charge. The integrated charge is detected with a fast (500 MHz bandwidth) sampling oscilloscope connected directly to the cathode. An absolute calibration is made with a calibrated charge-sensitive, low noise amplifier. The energy of the laser pulses is measured by calibrated photodiodes. The transmission of the optics and fused quartz viewport of the vacuum chamber is taken into account in calculating the pulse energy on the cathode. The laser spot area is measured with a linear photodiode array. The laser circular spot has a roughly Gaussian spatial energy distribution, and we used the FWHM radius of the laser spot (~0.8 mm) and FWHM temporal width (~500 fs) to calculate the peak intensity of the pulse.

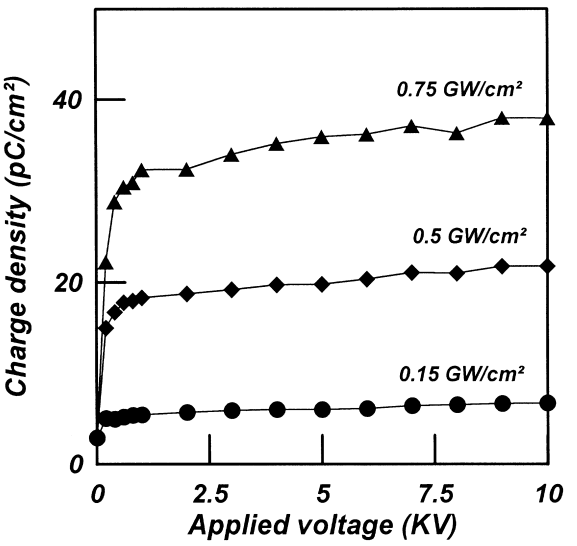

Fig. 1. Charge density versus applied anode voltage at different laser intensities. A saturation regime occurs for applied voltages larger than 8 kV.

3. Results and discussion

In Fig. 1 are reported measurements of the charge density versus the applied anode voltage V_A. An increasing extracted charge density, as a function of voltage, is observed for V_A of less than a few kV, a situation characteristic of the so called 'space charge limited' regime. At the other extreme, when $V_A>8$ kV, the curves become flat in all the measured intensity range, indicating that a saturation regime occurs, typical of a non-space charge-limited photoemission. The use of ultrashort laser pulses lead to a photoemission regime with strong space charge effects, due to the high charge density at the surface, so that the use of high dc electric fields is necessary to collect all the extracted charge. At the same time this prevents the measurements of the electrons energy spectra, as the information contained in the kinetic energy of the escaping electrons is blurred by the strong Coulomb interactions [13]. As a matter of fact, in these experiments, the total yield constitutes the primary information available on the photoemission process.

The intensity dependence of the total extracted charge density is presented in Fig. 2. Since the photon energy ($h\nu\cong4.7$ eV) is larger than the work function of Mo ($\Phi\cong4.6$ eV [14]), a single photon process is expected, with a total yield proportional to the peak laser intensity, as deduced from standard perturbation theory [15]. As evidenced in Fig. 2, a linear dependence of the yield on the intensity is observed only in the low intensity regime. For intensities higher than 0.1 GW/cm^2, the logarithmic slope N of the yield curve deviates from the value $N=1$, and increases with intensity. In Fig 3 is reported the photoelectric sensitivity dependence on intensity of the same data. The sensitivity S is measured in amperes per watt (A/W) and is defined

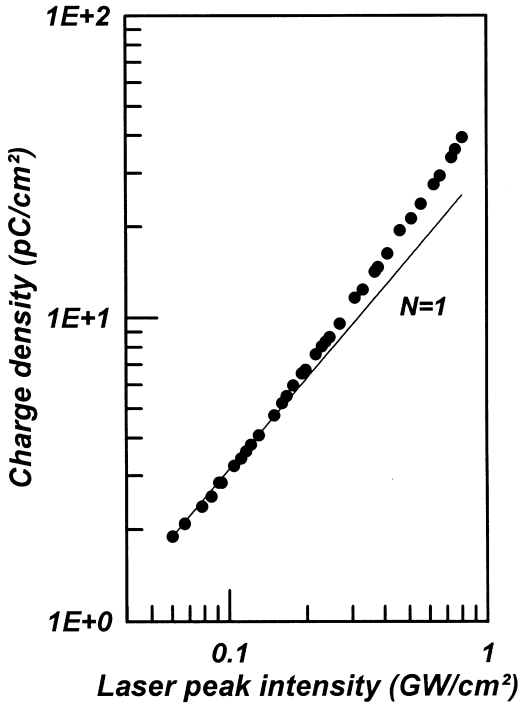

Fig. 2. Dependence of photoemitted charge density on peak intensity from a polycrystalline Mo sample. Laser pulse duration is 0.5 ps at a wavelength of 264 nm, beam is at normal incidence. Each point is on average over 100 laser shots.

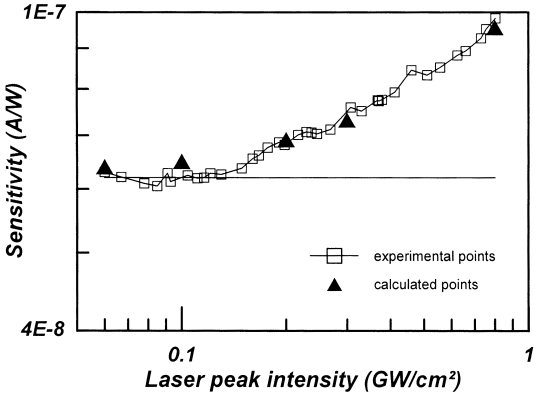

Fig. 3. Sensitivity versus peak intensity for a polycrystalline Mo sample. The experimental data are the same as in Fig. 2. Calculated points are derived from the TTM model and Eq. 4.

as J/I, where J is the peak current density and I is the laser peak intensity.

To explain the observed non-linearity in the total yield and sensitivity curve, as anticipated in the Introduction, the heating of the electrons induced by the laser pulses has to be considered. In the present experiment, the laser pulse temporal width ($\tau \cong 0.5$ ps) is shorter than the typical relaxation time between electron and phonons, that has been measured to be of the order of 1 ps for most metals [16]. Since the thermal capacitance of the lattice is at least two orders of magnitude higher than that of the electrons, the non-equilibrium heating process implies that electrons could reach relatively high peak temperatures when interacting with a sub-ps laser pulse even if the deposited energy per pulse is small (less than 10 μJ/pulse in this experiment).

According to EFD [4–7], the current density is expressed as a function of laser peak intensity and electron temperature as:

$$J_1 = a_1 \left[\frac{e}{h\nu}(1-R)I \right] A T_e^2 F(X_1)$$

$$X_1 = \frac{h\nu - \Phi}{k_B T_e} \tag{1}$$

where a_1 is a constant proportional to the transition probability of an electron from the conduction band to vacuum for the one-photon process ($N=1$, $h\nu - \Phi > 0$), A is the Richardson constant and F is the Fowler function. Using the parameters reported in Table 1, the single photon emission cross section a_1 for Mo at 264 nm is estimated to be 8×10^{-15} cm^2/A. The Fowler function, for $h\nu - \Phi > 0$, can be written as [6,7]:

$$F = F_0 - F_S \tag{2}$$

where

$$F_0 = \frac{\pi^2}{6} + \frac{X_1^2}{2}$$

$$F_S = \sum_{h=1}^{\infty} (-1)^{h+1} \frac{e^{-hX_1}}{h^2}. \tag{3}$$

The surface electron temperature profiles have been calculated using the two temperature model (TTM) [17,18]. The calculated electron peak temperatures, in the intensity range investigated here, do not

Table 1
Table of the physical constants

λ: Wavelength (nm)	264
R: Reflectivity[a]	0.66
K: Thermal conductivity[b] (W/m K)	142
C_l: Lattice heat capacity[c] (J/m^3 K)	2.65×10^6
γ: Electronic heat capacity[d] (J/m^3 K^2)	212
α: Absorptivity[e] (m^{-1})	18×10^7
g: Electron-phonon coupling[f] (W/m^3 K)	1×10^{17}
τ: Gaussian pulse width (FWHM) (s)	0.5×10^{-12}

[a] Measured at normal incidence.
[b] Ref. [19].
[d] Ref. [21].
[e] From $\alpha=4\pi k/\lambda$, Ref. [22].
[f] Refs. [23,24].
[c] Ref. [20].

exceed 600 K, which excludes a contribution from thermionic emission to the measured current density. Moreover, in the same intensity range, it satisfied the condition $k_B T_e < h\nu - \Phi$. As a consequence, the summation F_S is small with respect to F_0, and can be neglected, i.e. $F \approx F_0$. Under these conditions, the ratio between the non-linear, temperature enhanced, sensitivity (S) at high intensity levels and the linear photoelectric sensitivity (S_0) in the low intensity regime can be written as:

$$\frac{S}{S_0} = \frac{T_e^2 + \frac{3}{\pi^2}\left(\frac{\Delta}{k_B}\right)^2}{T_0^2 + \frac{3}{\pi^2}\left(\frac{\Delta}{k_B}\right)^2} \qquad (4)$$

where $\Delta = h\nu - \Phi$.

According to the present model, the ratio S/S_0 of the measured sensitivities is derived only from the (mean) surface electron temperature and the photon excess energy with respect to the work function (Δ). In this respect the total-yield photoemission data constitutes a direct probe of the non-equilibrium heating of the electron gas, and the approximate relation Eq. (4) gives the possibility to estimate directly the electron gas (non-equilibrium) temperature.

To verify the consistency of this theoretical framework, the TTM equations and Eq. (4) have been used to calculate the sensitivity enhancement in the same intensity range explored in the experiment. The temporal profile of the surface electron temperature induced by a 0.5 ps Gaussian laser pulse has been calculated using the set of parameters reported in Table 1. The measured sensitivity corresponds to an integrated charge and depends on the mean temperature $\langle T_e^2 \rangle^{1/2}$ of the electron gas, calculated by averaging the temperature profile in the FWHM temporal width of the laser pulse. In Fig. 3 are reported the values of the calculated sensitivity and the experimental values. A good agreement has been found for $\Delta = 80$ meV, implying a work function value $\Phi \approx 4.61$ eV, which is close to the value reported in [14] for polycrystalline Mo. An exact calculation, starting with Eq. (1) and integrating numerically the current J_1 gives a similar result, but in this case it is not possible to estimate the various parameters in so a simple way as from the approximate relation (Eq. 4).

References

[1] R. Yen, J.M. Liu, N. Bloembergen, T.K. Yee, J.G. Fujimoto, M.M. Salour, Appl. Phys. Lett. 40 (1982) 185.
[2] J.P. Girardeau-Montaut, C. Girardeau-Montaut, S.D. Moustaizis, C. Fotakis, Appl. Phys. Lett. 62 (1993) 426.
[3] J.P. Girardeau-Montaut, C. Girardeau-Montaut, Phys. Rev. B 51 (1995) 13560, and references therein.
[4] R.H. Fowler, Phys. Rev. 38 (1931) 45.
[5] L.A. DuBridge, Phys. Rev. 43 (1933) 727.
[6] J.H. Bechtel, W.L. Smith, N. Bloembergen, Phys. Rev. B 15 (1977) 4557.
[7] R. Yen, J. Liu, N. Bloembergen, Opt. Commun. 35 (1980) 277.
[8] R.M. Broudy, Phys. Rev. B 3 (1971) 3641.
[9] R. Danielius, A. Dubietis, A. Piskarskas, G. Valiulis, A. Varanavicius, Lithuanian J. Phys. 36 (1996) 329.
[10] H. Schulz, H. Schüler, T. Engers, D. von der Linde, IEEE J. Quantum Electron. 25 (1989) 2580.
[11] R. Yen, P. Liu, M. Dagenais, N. Bloembergen, Opt. Commun. 31 (1979) 334.
[12] M. Afif, J.P. Girardeau-Montaut, C. Tomas, M. Romand, M. Charbonnier, N.S. Prakash, A. Perez, G. Marest, J.M. Frigerio, Appl. Surf. Sci. 96–98 (1996) 469.
[13] M.V. Ammosov, J. Opt. Soc. Am. B 8 (1991) 2260.
[14] R.C. Weast, M.J. Astle (Eds.), Handbook of Chemistry and Physics, 63rd ed, CRC Press, Boca Raton, FL, 1982–1983.
[15] S.I. Anisimov, V.A. Benderskiĭ, G. Farkas, Sov. Phys. Usp. 20 (1977) 467, and references therein.
[16] S.D. Brorson, A. Kazeroonian, J.S. Moodera, D.W. Face, T.K. Cheng, E.P. Ippen, M.S. Dresselhaus, G. Dresselhaus, Phys. Rev. Lett. 64 (1990) 2172.
[17] M.I. Kaganov, I.M. Lifshitz, L.V. Tanatarov, Sov. Phys. JETP 4 (1957) 173.

[18] S.I. Anisimov, B.L. Kapeliovich, T.L. Perel'man, Sov. Phys. JETP 39 (1974) 375.
[19] C.J. Smithells (Ed.), Metals Reference Book, 5th ed.,, 1976.
[20] N.W. Ashcroft, N.D. Mermin, in: Solid State Physics, Saunders, Philadelphia, 1988, p. 428.
[21] P.B. Allen, Phys. Rev. B 36 (1987) 2920.
[22] E.D. Palik (Ed.), Handbook of Optical Constants of Solids, Academic Press, Orlando, FL, 1985.
[23] S.D. Brorson, A. Kazeroonian, J.S. Moodera, D.W. Face, T.K. Cheng, E.P. Ippen, M.S. Dresselhaus, G. Dresselhaus, Phys. Rev. Lett. 64 (1990) 2172.
[24] W.L. McMillan, Phys. Rev. 167 (1968) 331.